JOURNAL OF GEOPHYSICAL RESEARCH, VOL. 112, F03S17, doi:10.1029/2006JF000568, 2007

Using soil residence time to delineate spatial and temporal patterns of transient landscape response

Peter Almond,[1] Josh Roering,[2] and T. C. Hales[2]

Received 5 May 2006; revised 28 March 2007; accepted 8 May 2007; published 15 August 2007.

[1] On hillslopes the balance between soil transport and production determines local soil thickness and the age distribution of particles that comprise the soil (where age refers to the time elapsed since detachment from bedrock). The mean of this age distribution is defined as the residence time, and in a landscape with time-invariant topography (i.e., morphologic steady state), the spatial uniformity of soil production ensures that the residence time of soils is spatially invariant. Thus, given constant soil-forming factors, spatial variation of soil properties reflects differences in residence time driven by nonuniform soil production. Spatially extensive soil databases, which are often freely available in electronic form, provide a cheap and accessible means of analyzing patterns of soil residence time and quantifying landscape dynamics. Here we use a soil chronosequence to calibrate a chronofunction describing the reddening of soils in the Oregon Coast Range, which is then used to quantify the spatial distribution of soil residence time. In contrast to the popular conception that the Oregon Coast Range experiences uniform erosion, we observe systematic variations in soil residence time driven by stream capture, deep-seated landsliding, and lateral channel migration. Large, contiguous areas with short residence time soils (hue 10YR) occur west of the Siuslaw River–Long Tom Creek drainage divide, whereas soil patches with redder hues of 7.5YR or 5YR indicate longer residence times and transient landscape conditions. These zones of red soils (5YR) occur east of the Siuslaw–Long Tom divide, coinciding with low-gradient ridge and valley topography and deeply alluviated valleys resulting from drainage reversal in the Quaternary. Patches of red soils are also associated with deep-seated landslides at various locations in our study area. Our calculated soil residence times appear subject to overestimation resulting from limitations of the simple weathering index used here and chronofunction calibration uncertainties. Nonetheless, our soil residence time estimates appear accurate to within an order of magnitude and provide a useful constraint on landscape dynamics over geomorphic timescales.

Citation: Almond, P., J. Roering, and T. C. Hales (2007), Using soil residence time to delineate spatial and temporal patterns of transient landscape response, *J. Geophys. Res.*, *112*, F03S17, doi:10.1029/2006JF000568.

1. Introduction

[2] Having arrived in an unfamiliar landscape, one might ask the question: ''What features of the landscape carry the signature of steady or nonsteady conditions?'' Furthermore, one ponders, ''Given a suite of geomorphic features relevant to this question, to what temporal and spatial timescales do they speak?'' Recent developments in geochemistry have enabled the use of thermochronometers to compare exhumation rates with estimates of erosion rate [e.g., *Reiners et al.*, 2005]. Mountain ranges may tend toward steady state, defined as an approximate balance between rock uplift and erosion when integrated over timescales of 10^5–10^6 years [*Willett and Brandon*, 2002]. Alternatively, cosmogenic radionuclide (CRN) concentrations in stream sediment have been used to measure catchment-wide erosion rates over smaller spatial and temporal scales [*Bierman and Nichols*, 2004]. These estimates can similarly be compared to rock uplift constraints derived from marine terraces or in some cases fluvial strath terraces [*Pazzaglia and Brandon*, 2001]. On hillslopes, denudation rate measured from in situ bedrock CRN concentration can be used to constrain landscape lowering at the geomorphic process scale [*Heimsath et al.*, 2001a].

[3] These techniques are often expensive and time consuming. Although frequently overlooked in regional-scale geomorphic studies, soils are highly accessible and contain a wealth of information about landscape evolution. Much of the relevant data about the nature of surface materials, in fact, resides in soil reports and maps, and is freely available in electronic form. The reticence of geomorphologists to

[1] Soil and Physical Sciences Group, Division of Agriculture and Life Sciences, Lincoln University, Canterbury, Christchurch, New Zealand.
[2] Department of Geological Sciences, University of Oregon, Eugene, Oregon, USA.

0148-0227/07/2006JF000568$09.00

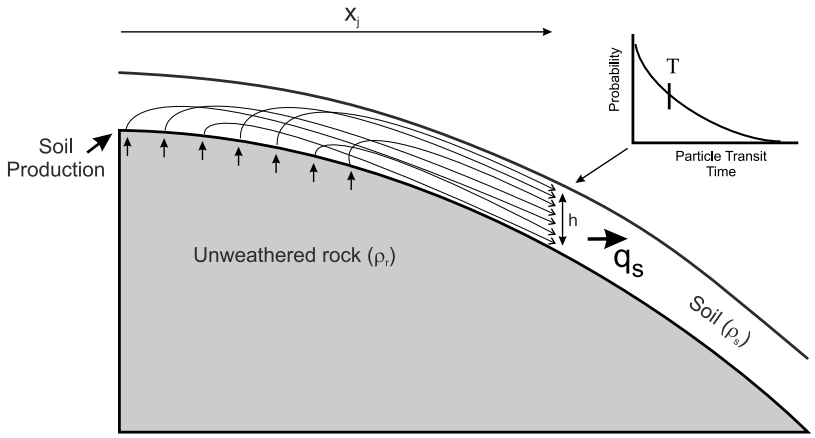

Figure 1. Soil residence time model. The residence time of the soil at a distance, x_j, from the ridge crest is the average of transit times for all soil particles since detachment from bedrock. Chemical weathering is assumed to start once a particle becomes incorporated in the actively transporting layer of thickness, h. At any location along the slope the mean of the particle age distribution (i.e., residence time) is independent of slope position on a steadily eroding hillslope.

mine soil data may result from the perception that pedology is preoccupied with the vertical differentiation of soils into horizons, and therefore has little to offer those concerned with multidimensional processes associated with landscape evolution. The discipline of soil geomorphology, however, has long focused on the genetic relationships between soils and landscapes [*Holliday*, 2006]. A common theme has been to use soils as a relative or calibrated age dating tool [*Noller et al.*, 2000]. Chronofunctions developed from soil chronosequences, which relate soil properties to soil age, can be used to date landforms of unknown age via the soils that mantle them. Most studies of this kind involve landforms, either erosional or constructional, for which a simple relationship exists between soil and landform age. For example, soils have been used to date fluvial terraces and fans [*Bull*, 1991], moraines [*Birkeland*, 1999], dunes [*Wells et al.*, 1990] and marine terraces [*Bockheim et al.*, 1992]. In these cases soil age has a simple interpretation, the time of cessation of deposition or erosion.

[4] Few studies have used soils to date or investigate dynamics of hillslopes. *Mills* [2005] interpreted variations in the soil weathering across hollows and noses on Appalachian valley slopes in terms of valley slope evolution. *Tonkin and Basher* [1990] used chronofunctions calibrated from radiocarbon and weathering rind dating, in association with stratigraphic principles, to assess the residence time of soil on hill and mountain slopes along a transect across the Southern Alps of New Zealand. Their approach, heavily influenced by the soil periodicity concepts of *Butler* [1982], assumed erosion events (shallow landsliding) periodically removed the soil mantle, after which soil formation started anew. Soil residence time, interpreted as the length of time since the slope stabilized, was estimated from an appropriate chronofunction. *Birkeland* [1999] used chronofunctions and the spatial distributions of soil orders to estimate maximum denudation rates for the Colorado front range of the Rocky Mountains. The denudation rate could be no greater than that which allowed the typical thickness of a given soil order to persist during soil formation. For example, if Alfisols take 10,000 years to form and soil thickness is typically 1 m, then denudation rate must be less than 0.1 m kyr^{-1}. Although not explicitly stated, *Birkeland* [1999] appear to adopt a conceptual framework in which denudation and soil formation (production) act simultaneously. In such a situation, soil age as typically defined has limited relevance because the soil is composed of particles with a distribution of ages (defined by the time elapsed since their incorporation into the soil mantle). The residence time is the average of this age distribution [*Anderson et al.*, 2002; *Mudd and Furbish*, 2006; *Small et al.*, 1999].

[5] Here we develop an analytical model for soil residence time and use soil properties mapped in a 1:20,000 county soil survey calibrated against a soil chronosequence to estimate the residence time of soils on hillslopes in the Oregon Coast Range (OCR). The melding of these two data sets will enable us to both test hypotheses of steady state and infer geomorphic drivers of transient landscape behavior. We extend the approach of *Birkeland* [1999], by considering soil at a point on a hillslope as comprising the flux of colluvial material with an age distribution determined by the transit times of individual soil particles (Figure 1). In this context, we then define the residence time as the flux-weighted average of the component transit times [*Bolin and Rodhe*, 1973]. Because the spatial distribution of soil residence time for a given landscape reflects the balance between soil production and transport, soil properties can provide spatial constraints on landscape dynamics and the tendency for denudation to balance rock uplift. For landscapes in morphologic steady state and with spatially uniform rock uplift, soil residence time should be everywhere equal. Thus, accepting the soil forming factor paradigm of *Jenny* [1941], in the absence of variations in parent material, biology, climate, or topographically induced changes in soil drainage, morphologic steady state will manifest as a spatially uniform soil mantle. In

contrast, spatial variation in soil properties implies transient conditions.

2. Model for Soil Residence Time and Pedogenic Alteration on Hillslopes

[6] In an erosional landscape everywhere incising at the same rate, a balance exists between mass delivered by rock uplift and that removed by erosion. Morphological steady state [*Willett and Brandon*, 2002] occurs when erosion rate is everywhere equal to rock uplift rate and topography becomes temporally invariant. For a steady state, soil-mantled hillslope with spatially uniform erosion (E), the one-dimensional flux of soil, q_s, at distance x from the hill crest, is given by

$$q_s = E\frac{\rho_r}{\rho_s}x, \tag{1}$$

where ρ_r is the density of rock, and ρ_s is the density of soil. The depth-averaged velocity of soil is given by

$$v_x = \frac{q_s}{h}, \tag{2}$$

where h is the depth of soil (Figure 1). Assuming well mixed soil, a particle of rock detached by physical weathering processes (i.e., soil production) at x moves at velocity v_x:

$$v_x = \frac{E}{h}\frac{\rho_r}{\rho_s}x. \tag{3}$$

The soil at any point on the slope is made up of particles of weathered rock detached from all points upslope to the hillcrest (Figure 1). The transit time t_i for a particle detached at point x_i to reach a location downslope, x_j, is given by

$$t_i = \int_{x_i}^{x_j}\frac{dx}{v_x} = \frac{\rho_s}{E\rho_r}\int_{x_i}^{x_j}h\frac{dx}{x}. \tag{4}$$

Assuming the depth of actively transporting soil to be constant,

$$t_i = \frac{h}{E}\frac{\rho_s}{\rho_r}\int_{x_i}^{x_j}\frac{dx}{x} = \frac{h}{E}\frac{\rho_s}{\rho_r}\ln\frac{x_j}{x_i}. \tag{5}$$

The ensemble of particles comprising the soil at x_j includes particles with ages determined by their transit times, and those ages are given by

$$t = \frac{h}{E}\frac{\rho_s}{\rho_r}\ln\frac{x_j}{x} \quad \text{where } 0 < x \le x_j. \tag{6}$$

Because t is determined by the ratio x_j/x, it depends on travel distance and relative position along the slope; that is, the travel time of a particle going from x = 2 to 4 m is the same as that for a particle going from x = 4 to 8 m. The average particle age, which is defined as the residence time, T, is independent of position and is given by the flux-weighted sum of the individual particle transit times divided by the total flux (Figure 1):

$$T = \frac{h}{E}\frac{\rho_s}{\rho_r}\frac{\int_0^{x_j}\ln\left(\frac{x_j}{x}\right)Edx}{Ex_j} = \frac{h}{E}\frac{\rho_s}{\rho_r x_j}\left[x\left(\ln\left[\frac{x_j}{x}\right]+1\right)\right]_0^{x_j} = \frac{h}{E}\frac{\rho_s}{\rho_r}. \tag{7}$$

This result is equivalent to a previous study [*Mudd and Furbish*, 2006] and demonstrates the spatial invariance of average soil particle age (or residence time) along steady state hillslopes. Furthermore, *Mudd and Furbish* [2006] show that the probability density function for the distribution of particle ages is an exponential function (Figure 1), such that at a given location, relatively few particles have been traversing the slope for a long period of time.

[7] If the extent of pedogenic alteration, $W(t)$, as measured by the degree of chemical alteration, follows a generic function of time, then the alteration of a soil particle upon reaching x_j and having been detached from bedrock at x_i is given by

$$W_i = W\left(T\ln\left[\frac{x_j}{x_i}\right]\right), \tag{8}$$

where the expression in parentheses is the argument of the function, which equates to the transit time of the particle from x_i to x_j (as defined by equations (6) and (7)). Thus the weathering of a soil particle depends on the spatially invariant residence time and relative position along the slope. Similarly, the mean degree of alteration for the column of soil at x_j, is the flux-weighted average degree of alteration for particles derived from all upslope points:

$$\overline{W}_{x_j} = \frac{\int_0^{x_j}W\left(T\ln\frac{x_j}{x}\right)Edx}{Ex_j} = \frac{\int_0^{x_j}W\left(T\ln\frac{x_j}{x}\right)dx}{x_j}. \tag{9}$$

Now, we can substitute a time-dependent weathering function into equation (9) to determine how the extent of weathering varies in our steady state system. Consider an exponential weathering function of the following form:

$$\mathrm{W}(t) = W_0 + K\left(1 - e^{-\lambda t}\right), \tag{10}$$

where W_0, K, and λ describe the weathering response (e.g., chemical alteration) of a soil particle with time. In equation (10), W_0 and K have units equivalent to the particular weathering variable and λ has units of T^{-1}. Substituting equation (10) into equation (9) gives

$$\begin{aligned}\overline{W} &= \frac{\int_0^{x_j}\left[W_0 + K\left(\left(1 - e^{-\lambda T\ln\frac{x_j}{x}}\right)\right)\right]Edx}{Ex_j}\\ &= \frac{\int_0^{x_j}(W_0+K)dx - K\int_0^{x_j}\left(\frac{x_j}{x}\right)^{-\lambda T}dx}{x_j}.\end{aligned} \tag{11}$$

Carrying out the integration, we obtain

$$\overline{W} = \frac{(W_0 + K)x\big|_0^{x_j} - Kx_j^{-\lambda T}\frac{x^{\lambda T+1}}{\lambda T+1}\Big|_0^{x_j}}{x_j}, \tag{12}$$

which simplifies to the following relationship:

$$\overline{W} = W_0 + K - K\frac{1}{\lambda T+1} = W_0 + K\frac{\lambda T}{\lambda T+1}. \tag{13}$$

Equation (13) describes the spatially invariant state of soil weathering on hillslopes in morphologic steady state and can be rearranged as

$$T = \frac{\overline{W} - W_0}{\lambda\left(K - \left[\overline{W} - W_0\right]\right)}, \tag{14}$$

which provides a basis for estimating residence time at the local hillslope scale if a function describing the evolution of soil weathering can be determined and the spatial variation of soil properties is known. Many chronofunctions similar to equation (10) have been derived [e.g., *Birkeland*, 1999]; these functions can be used as a calibrated dating technique so long as soil-forming factors remain similar to the chronofunction calibration site. Most chronosequence studies that apply this methodology select stable landforms, such as terraces, moraine crests, or fan surfaces, in order to eliminate the effect of erosion and isolate the effect of time on soil development. As a result, such chronofunction studies apply to soils comprising particles of uniform age. The significance of equation (14) is that, by accounting for the age distribution of soil particles that constitute steady state hillslope soils, it enables us to use a chronofunction derived from stable-landform chronosequences to estimate soil residence time on eroding hillslopes.

3. Study Area

[8] The Oregon Coast Range (OCR) is a humid, soil-mantled, mountainous landscape largely composed of Eocene sedimentary rocks that overlie volcanic basement accreted to the North American plate in the early Tertiary [*Orr et al.*, 1992]. Located atop the overriding North American Plate of the Cascadia subduction zone, the OCR constitutes a forearc high in the orogenic wedge model proposed by *Brandon* [2004]. According to this structural model, continuing convergence of the Juan de Fuca Plate and associated accretion causes underplating and uplift of the coastal ranges. Uplift and vertical exhumation within the forearc high are separated from a topographic low to the east by the retro–shear zone. In this case, the north-south trending Willamette Valley corresponds to the topographic low, although structures defining the retro–wedge margin are currently undefined [*Yeats et al.*, 2000] (Figure 2). An alternative model proposed by *Wells et al.* [1998] emphasizes the dynamics of large blocks in regulating the tectonic evolution of western Oregon, including the boundary between the Oregon Coast Range and the associated extensional regime along the crest of the Cascade Range. The Quaternary evolution of the forearc high may have profound implications for reconstructing the course of western Oregon river systems as preliminary data suggest that the Willamette Valley may be migrating south, capturing Cascade-draining rivers in its wake [*Baldwin and Howell*, 1949; *Chylek*, 2002; *Moeller*, 1990].

[9] Our study area is roughly coincident with the Siuslaw drainage basin whose headwaters terminate just south of the southern extension of the Willamette Valley (Figure 2). The area is almost exclusively underlain by the Tyee Formation, which has been studied in detail because of its distinct assemblage of sedimentary facies [*Chan and Dott*, 1983; *Heller and Dickinson*, 1985; *Lovell*, 1969]. *Heller and Dickinson* [1985] suggested that the Tyee Formation is a sand-rich sequence of turbidite deposits originated from a delta-fed submarine ramp depositional system. Since the late Eocene, the Tyee Formation has been compressed into a series of low-amplitude, gently dipping folds (the maximum dip of bedding along the flanks of folds rarely exceeds 15–20°) oriented north-northeast [*Baldwin*, 1956]. Uplift of the OCR commenced in the Miocene [*McNeill et al.*, 2000] and continues today as evidenced by abandoned wave-cut platforms along the Oregon Coast [*Kelsey et al.*, 1996]. Rates of rock uplift derived via dating of marine terraces adjacent to our study area (latitude ranging from 43° to 45°) vary from <0.1 to 0.3 mm yr^{-1} [*Kelsey et al.*, 1996] and are generally an order of magnitude lower than geodetic uplift rates derived from highway leveling and tide gauge data [*Mitchell et al.*, 1994]. Both short- and long-term uplift rates measured along the coast vary locally owing to vertical movement along faults, although it is unclear whether these local variations extend a significant distance inland.

[10] The topography of the OCR has been characterized as steep and highly dissected with relatively uniform ridge and valley terrain [*Dietrich and Dunne*, 1978; *Montgomery*, 2001; *Reneau and Dietrich*, 1991]. Typically, soil is relatively thin (~0.4 m) on hilltops and sideslopes and thicker (~1–2 m) in unchanneled valleys that act as preferential source areas for shallow landslides that often initiate debris flows [*Dietrich and Dunne*, 1978; *Heimsath et al.*, 2001a]. Most studies of decadal- to millennial-scale patterns of sediment production and delivery in the OCR have focused on the cyclic infilling and evacuation of soil in steep, convergent areas [*Benda and Dunne*, 1997; *Dietrich and Dunne*, 1978; *Reneau and Dietrich*, 1990]. Erosion rates generated by short- (~10 years) and long-term (~5000 years) analyses of sediment yield are 0.10–0.15 mm yr^{-1} [*Beschta*, 1978; *Bierman et al.*, 2001; *Heimsath et al.*, 2001b; *Reneau and Dietrich*, 1991], consistent with rates of coastal uplift [*Kelsey et al.*, 1996] and Holocene bedrock channel incision [*Personius*, 1995]. These studies have been used to argue that an approximate balance exists between rock uplift and erosion in the OCR such that the topographic form may be relatively uniform with time [*Montgomery*, 2001; *Reneau and Dietrich*, 1991; *Roering et al.*, 1999]. This interpretation should be tempered, however, by the uncertainty in extrapolating uplift rates generated via marine terraces to inland areas. Short, steep hillslopes that erode via nonlinear slope-dependent processes can rapidly (~40 ka) adjust their morphology to climatic or tectonic perturbations [*Roering et al.*, 2001], enabling a tendency toward steady state erosion. In contrast, deep-seated landslides [*Roering et al.*, 2005], fluvial terrace

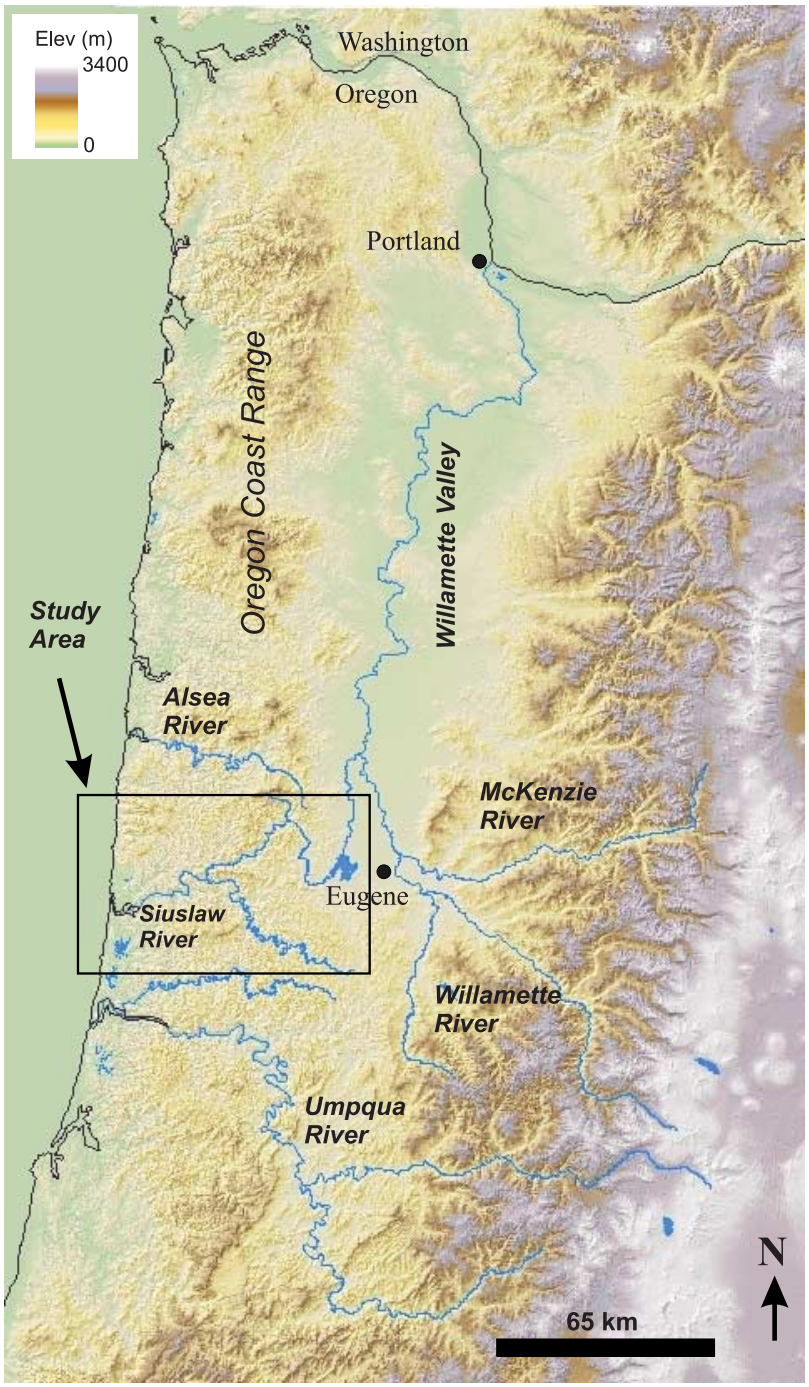

Figure 2. Shaded relief map of the Oregon Coast Range and Willamette Valley. This map shows the major topographic and hydrologic features of the region, including the Oregon Coast and Cascade Ranges separated by the low topography of the Willamette Valley. The Willamette River gathers much of the drainage from the Cascade Range and sends it northward to the Columbia River. South of the Willamette River drainage the Umpqua River drains both the Cascade and Oregon Coast Range and may be an analogue for the Siuslaw River before capture by the Willamette River. Our study area focuses on the Siuslaw River basin, situated at the southern terminus of the Willamette Valley.

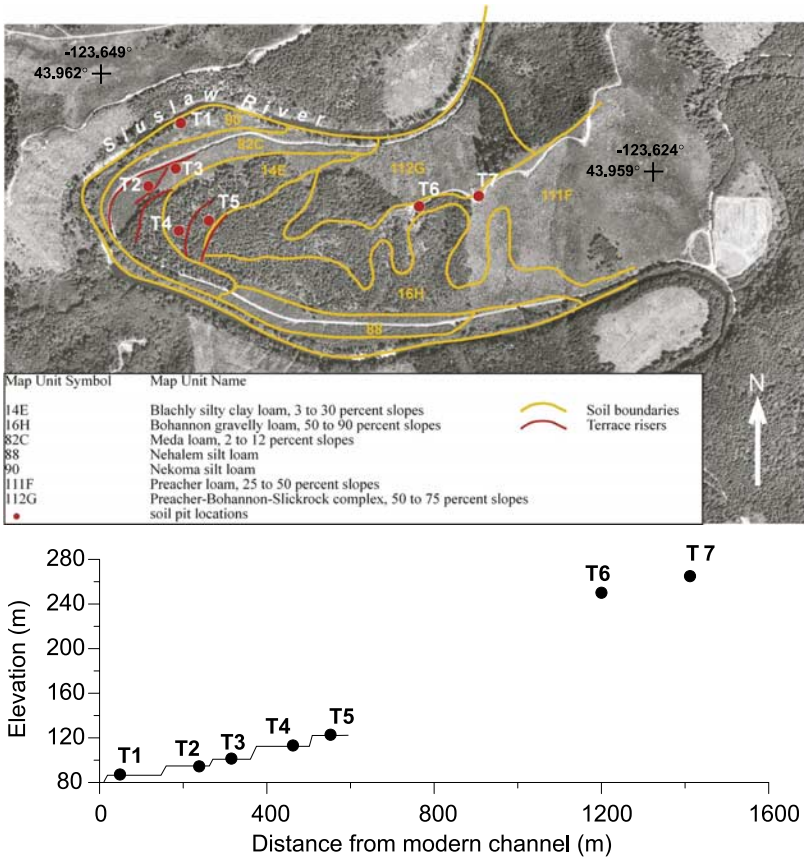

Figure 3. Map of terrace location and terrace profile for the soil chronosequence. Terrace risers (red lines) and soil pit locations (red dots) represent sites of detailed soil description, while the yellow lines represent soil-mapping units of the Lane County Soil Survey [*Patching*, 1987]. Orthophoto base was derived from NASA World Wind software.

remnants, and debris flow fans produce topographic features that persist for 10–100 ka and temporal patterns of sediment production associated with these features are unconstrained.

4. Methods

4.1. Soil Chronosequence

[11] We defined a soil chronosequence from a flight of five fluvial terraces along a ridge formed on the inside of a meander along the Siuslaw River (Figure 3). The lowest terrace tread was 5 m above the modern channel floor and may in fact represent the present floodplain. Nevertheless, hereafter, we retain the designation Terrace 1 for this surface. The terrace treads became narrower with increasing elevation above the channel. Above Terrace 5, we observed minimal morphological expression of terraces but two flat, narrow (~10–15 m) steps along the ridgeline coincided with patches of deep, very red soils, continuing the pattern of soil evolution displayed across the lower five terraces. We considered these soils to be remnants of weathering profiles that began forming on terraces now heavily modified by lateral erosion on either side of the ridgeline. Soils were described from pits excavated to at least 1.4 m depth on the lower five terraces, and from roadside exposures on the upper two ridgeline steps. A bucket auger was used to sample below the base of the pits or exposures to hard bedrock. At both ridgeline step sites soft, clayey saprolite extended beyond the 8 m depth limit of the auger we used. Soil description followed the methods of *Milne et al.* [1995].

[12] Surface elevations for the upper two soils (Terraces 6 and 7) were surveyed by differential GPS with an estimated uncertainty of ±0.5 m. Using a GPS-derived datum on Terrace 5, we surveyed the elevation of soil pits on Terraces 1–4 with a total station to achieve ~0.2 m accuracy. We established the terrace chronology by radiocarbon dating detrital charcoal from soil pits in Terraces 1 and 2 and using the resulting incision rate to estimate ages for Terraces 3–7 based on the elevation of the terrace strath above the modern strath. Radiocarbon ages were converted to calendar years using the IntCal04 calibration data set [*Reimer et al.*, 2004] as implemented in Calib 5.0.1 [*Stuiver and Reimer*, 1993]. Where incision is continuous this method will tend to overestimate soil age because it does not account for aggradation. If aggradation is relatively short-lived as we expect, the error is minimal for all but the youngest terraces. On the ridgeline terrace remnants, a boundary between an upper biomantle and a lower zone retaining bedrock fabric could be identified, but because of the erosional nature of these sites we could not be sure whether the boundary

represented the strath or a downward moving soil boundary somewhere below the original strath. For these sites we used differences in elevation of soil surface to present strath, acknowledging potential for age underestimation.

4.2. Calculation and Mapping of Soil Residence Time

[13] We undertook a four-step process to quantify soil residence time in our study area. They were (1) derive a chronofunction to calibrate soil morphological evolution in terms of soil age, (2) extract the relevant soil morphological data from soil survey map unit and taxonomic unit descriptions, (3) convert morphological data to residence time using the parameters of the chronofunction in equation (14), and (4) map residence time using a Geographic Information System. A simple, univariate index of reddest hue in the B horizon was adopted to quantify soil development and establish a soil chronofunction. We used an exponential function of the form given in equation (10) to calibrate the hue-terrace age relationship and estimate values of W_0, K, and λ. Soil hues were converted to hue numbers such that each major change in Munsell hue (e.g., 10YR to 7.5YR) corresponded to an increment of 2.5 hue units. A hue number of 0 was assigned to 2.5Y with redder hues increasing monotonically.

[14] The rationale for adopting a simple, univariate chronofunction based on soil hue is as follows: (1) Color change was the most significant and systematic change in soil morphology across the sequence. Soil textures also changed systematically, but above Terrace 4, clay percentage became relatively constant. (2) Other morphological data (such as soil structure, depth of horizons, and weathering of clasts) were either not recorded in the soil survey soil descriptions, or would have introduced bias because of qualitative observational differences between the practitioners (i.e., this study and the soil surveyors). (3) A sophisticated multivariate index was not justified given that only one typical or modal soil profile description in the soil survey report was provided to characterize each (spatially variable) soil delineation.

[15] We used the Lane County soil survey database [*Patching*, 1987] to identify the hue of mapped soils units and map soil residence time via our soil chronofunction and equation (14). The resulting map included the terrace flight used for our soil chronosequence, enabling us to compare our field observations with the soil map.

[16] Because soils of the chronosequence were well drained and formed in alluvium derived from the Tyee formation, we restricted our analysis of residence time to soil map units on hillslopes with related parent materials (sandstone or sandstone and siltstone). We did not include soil units associated with terraces, fans, and other valley floor landforms because the potential for soil drainage influences on soil color was high, and because the age of soils on these landforms is not directly related to hillslope dynamics. Furthermore, such units constitute a negligible fraction of our study area (<0.5%). We also excluded topographic hollows and low-order drainages within the hillslope soil-mapping units because these landforms do not satisfy the assumptions of our model. In contrast to the steady state between soil production and net transport assumed to apply on hillslopes, such convergent zones have been shown to be sites of episodic accumulation of a thick colluvial infill, and subsequent evacuation [*Dietrich and Dunne*, 1978; *Reneau and Dietrich*, 1991]. We used a 10-m DEM of the study area and a drainage area estimation algorithm [*Tarboton*, 1997] to map the extent of the low-order channel and "hollow" network. In the OCR, the transition between hillslopes and the valley network is well described by a threshold contributing area per unit contour width (a/b), whereby larger values tend to be associated with topographic convergent zones. We identified portions of the terrain with a/b values greater than 50 m (as defined by *Roering et al.* [2001]) and excluded them from our analysis. As expected, these convergent zones comprise a relatively small proportion of the landscape (<7%), and their density was relatively consistent across the study site.

[17] Most of the soil map units established on Tyee Formation were identified as simple map units; that is, the delineations were deemed to be dominated by a single soil taxonomic unit (soil series). From the descriptions of the soil series corresponding to each of the simple map units, we tabulated the yellowest hue in the B horizon from the range of hues given (e.g., 10YR to 7.5YR). We selected the yellowest extreme because our own and other workers' observations of the dominant soil hue (Bohannon, Digger, Preacher soils) on OCR hillslopes corresponded with the yellow end-member quoted in the soil series descriptions. We acknowledge that this may tend to underestimate our estimates of soil residence time. To identify regional patterns in soil properties associated with tectonic forcing or other factors, we used ArcMap GIS to quantify spatial variation in soil hue (and thus residence time) across our study area.

5. Results

5.1. Soil Chronosequence

[18] A 2.5 m deep pit on Terrace 1 exposed the surface soil and four buried soils formed in sandy alluvium. The surface soil was an Entisol [*U. S. Natural Resources Conservation Service*, 1999] showing rudimentary soil development. A 10-cm-thick A horizon overlay a weak or loose, brown (10YR 4–5/3), structureless medium sand (C horizon) with its base at 40 cm depth (Table 1). The brown color of the C horizon despite the lack of any other signs of pedogenic alteration suggests the sediment carried by the Siuslaw River is weathered during transport down hillslopes. Colors taken from unweathered Tyee sandstone bedrock around the catchment were olive grey (5Y 4–5/2) whereas the dominant hue in hillslope soils is 10YR. The first and fourth buried soils had dark A horizons and relatively bright (10YR 4/6) B horizons characteristic of Inceptisols. The second and third buried soils had duller (yellowish brown) B horizons showing weak soil structure, and paler A horizons. Below 3.2 m depth to the strath at 6.2 m the sediment showed no signs of pedogenic alteration. Radiocarbon ages from charcoal have provided some constraints on the timing of aggradation and the duration of pedogenesis. A sample of detrital charcoal from 6.15 m depth within a thin veneer of gravel on the strath yielded a radiocarbon age of 4,449 ± 51 ^{14}C yr BP (AA67948, University of Arizona AMS), constraining the cumulative duration of pedogenesis for all soils to ca 5000 calendar years (cal years). In situ charcoal from a carbonized root at 1.75 m

Table 1. Data Set for Terraces 1–7[a]

	Terrace 1	Terrace 2	Terrace 3	Terrace 4	Terrace 5	Terrace 6	Terrace 7
Tread elevation, m	85.5	89.0	94.3	106.9	117.6	248.9	263.8
Depth to strath	6.2	2.3	2.6	2.5	2.2	n.m.	n.m.
Present strath elevation, m	79.3	79.3	79.3	79.3	79.3	79.3	79.3
Elevation difference, m							
Strath to strath	0.0.	7.3	12.4	25.1	36.1	n.a.	n.a.
Soil surface to strath	—	—	—	—	—	163.4	178.3
Inferred age, ka	3.5[b]	30[b]	69[c]	140[c]	200	908	990
Reddest hue	10YR	10YR	5YR	5YR	2.5YR	10R	10R
Base of B horizon,[d] cm	N.A.	88	113	240	400	350	450
Base of weathering,[e] cm	—	109	260	310	460	910+	1100+

	Terrace 1		Terrace 2		Terrace 3		Terrace 4		Terrace 5		Terrace 6		Terrace 7	
	Depth, cm	Soil Descr.	Depth, cm	Soil Descr.	Depth, cm	Soil Descr.	Depth, cm	Soil Descr.	Depth, cm	Soil Descr.	Depth, cm	Soil Descr.	Depth, cm	Soil Descr.
Horizon 1	−2 to 0	L, F, H	−4 to −2	L	−4 to 0	L, F, H, 10YR 2/1	−5 to 0	H, 10YR 2/1	−2 to 0	L, F, H	−8 to 0	spoil	−2	L
Horizon 2	0–10	A, ms, 10YR 3/2	−2 to 0	H, 10YR 2/1	0–28	A, zl, 10YR 4/2, str fi nt, f mod wthd grv	0–28	A, zl, 7.5YR 3/2, str fi nt, f mod wthd grv	0–21	A, zl, 5YR 3/2, str fi nt	0–8	A, zc, 10YR 3/4, mod med + co bk	0–20	A, cl, 5YR 3/4, str v fi nt,
Horizon 3	10–25	C, ms, 10YR 4/3, wk med nt	0–7	A, zl, 10YR 3/2, mod fi nt	28–44	Bw1, zl, 10YR 4/3, mod fi + med nt, f mod wthd grv	28–42	Bw1, cl, 5YR 4/3, str fi + med nt, f cont c cutans, com h wthd grv	21–50	Bw, sli stn cl, 5YR 4/4, str fi + med nt, f mod wthd st	8–39	AB, zc, 2.5YR 4/4, mod fi + med nt	20–37	Bw, zc, 2.5YR 3/4, str fi nt
Horizon 4	25–35	2C, ms, 10YR 5/3	7–38	Bw1, zl, 10YR 4/2, str fi nt	44–68	Bw2, zl, 7.5YR 4/4, mod fi bk, com ptch c cutans, f mod wthd grv	42–75	Bw2, sli grvly + bldy cl, 5YR 4/6, mod fi + med bk, com ptch c cutans, com h wthd grv	50–100	Bt1, cl, 2.5YR 3/6, wk co bk, com cont c cutans	39–92	Bt1, zcl, 10R 4/6, mod co bk, m cont c cutans	37–73	Bt, zc, 2.5YR 3/6, mod co bk, m cont c cutans
Horizon 5	35–40	3C, ms, 10YR 4/3, wk med bk	38–88	Bw2, zl, 10YR 3/3, mod med bk, f mod wthd grv	68–113	Bt, zl, 5YR 4/4, wk med bk, com disc c cutans	75–120	2Bt, sli bldy zl, 5YR 4/4, mod fi + med bk, m ptch c cutans, com mod wthd bld	100–150	Bt2, sli grv cl, 2.5YR 4/6, str med bk, m cont c cutans	92–200	Bt2, zcl, 2.5YR 3/6, mod med bk, m cont c cutans	73–140	2Bt1, zc, 10R 4/6, str med prs, ab cont c + ox cutans

Table 1. (continued)

	Terrace 1		Terrace 2		Terrace 3		Terrace 4		Terrace 5		Terrace 6		Terrace 7	
	Depth, cm	Soil Descr.	Depth, cm	Soil Descr.	Depth, cm	Soil Descr.	Depth, cm	Soil Descr.	Depth, cm	Soil Descr.	Depth, cm	Soil Descr.	Depth, cm	Soil Descr.
Horizon 6	40–53	4bA1, 10YR 3/1, wk fi nt	88–109	BC, zl, 2.5Y 5/4, mod med bk	113–200	BCt, zl, 7.5YR 4/4, wk med bk, com disc c cutans, f mod wthd grv	120–150	2Bw, mod gvly + stny zl, 7.5YR 5/6, wk co bk, com disc c cutans, com h wthd grv	—	—	—	—	140–190	2Bt2, zc, 2.5YR 5/6, mod med + co bk, m cont c cutans
Horizon 7	53–75	4bA2, sl, 10YR 3/3, mod med nt	109–122	C1, zl, 2.5Y 6/4, wk med bk	—	—	—	—	—	—	—	—	190–270	2Bt3, zcl, 2.5YR 5/6, mod co bk, m disc c cutans
Horizon 8	75–87	5bBw, ms, 10YR 4/6, wk med bk	122–146	C2, sli grv zl, 5Y 6/2, f med dist 5YR 4/6 mottles, mass, f mod wthd grv	—	—	—	—	—	—	—	—	—	—
Horizon 9	85–107	5bC, ms, 10YR 4/4	—	—	—	—	—	—	—	—	—	—	—	—
Horizon 10	107–125	6b2Bw/Acum, sl, 10YR 4/4, mod fi + med nt	—	—	—	—	—	—	—	—	—	—	—	—
Horizon 11	125–147	6b3A, zl, 10YR 4/3, mod fi + med nt	—	—	—	—	—	—	—	—	—	—	—	—
Horizon 12	147–166	6b3Bw, sl, 10YR 5/4, mod med bk	—	—	—	—	—	—	—	—	—	—	—	—
Horizon 13	166–187	6b4A, sl, 10YR 3/3, mod med bk	—	—	—	—	—	—	—	—	—	—	—	—
Horizon 14	187–191	6b4A/B, sl, 10YR 4/3, mod med bk	—	—	—	—	—	—	—	—	—	—	—	—
Horizon 15	227–250	9b4Bw, sl, 10YR 4/6, mod co bk	—	—	—	—	—	—	—	—	—	—	—	—

[a]Abundance: f, few; com, common; m, many; ab, abundant. Texture modifiers: sli, slightly; mod, moderately; v, very; grv, gravelly; stn, stony; bldy, bouldery. Texture class: s, sand; ms, medium sand; sl, sandy loam; zl, silt loam; cl, clay loam; zcl, silty clay loam; zc, silty clay; c, clay. Size terms: fi, fine; med, medium; co, coarse. Mottle distinctness: fnt, faint; dist, distinct; prom, prominent. Structure grade: wk, weak; mod, moderate; str, strong. Structure type: nt, nutty; bk, blocky; prs, prismatic; mass, massive; sg, single grain. Cutan continuity: cont, continuous; disc, discontinuous; ptch, patchy. Cutan type: c, clay; c + ox = clay/oxide. Clast weathering: sli wthd, slightly weathered; mod wthd, moderately weathered; h wthd, highly weathered. Clast size: grv, gravels; st, stones; bld, boulders.

[b]Based on radiocarbon.

[c]Based on an uplift rate of 0.18 mky^{-1} calculated from Terrace 2.

[d]Defined at the lower limit of the presence of pedological features such as soil structure and clay cutans and absence of rock or sedimentary fabric.

[e]Defined as the boundary between oxidized and unoxidized sediment or the boundary between soft, weathered rock and hard unweathered rock.

within the A horizon of the fourth buried soil returned a radiocarbon age of 3323 ± 39 ^{14}C years BP (AA67947, University of Arizona AMS) and a 2σ calibrated age of 3455 to 3640 cal years BP. Together these ages establish a minimum duration of pedogenesis of the fourth buried soil to ca 1500 cal years. The similarity of B horizon hue between the first and fourth buried soils suggests that the formation of these two soils represents a major part of the time since aggradation. Because on this terrace sedimentation and pedogenesis occurred in alternating episodes, the ca 5000 years of pedogenesis, as represented by soil development, is dispersed over multiple soils.

[19] Soils on higher terraces, except perhaps Terrace 4, were apparently unisequal, although it may be that long periods of pedogenesis have overwhelmed any prior soil stratigraphy [*Ruhe and Olson*, 1980] to give the appearance of simplicity. On Terrace 2 the soil was an Inceptisol with a thin dark greyish A horizon, characteristic of forest soils, over a dark greyish brown to dark brown (10YR 4–3/2–3) B horizon with strong to moderately developed structure. The texture of the soil was a silt loam, distinctly finer than that of Terrace 1. The pale color of the C horizon compared to the browner colors of C horizons on Terrace 1 probably relates to reduction of iron due to poor drainage as indicated by the mottles in the lower subsoil. Two radiocarbon samples between 1.80 and 2.26 m depth produced ages of 2239 ± 42 and 34,340 ± 810 ^{14}C years BP (AA66858 and AA66857, University of Arizona AMS), respectively. The younger age likely arises from in situ charcoal incorporated to depth by bioturbation. The deeper sample is much more likely to be detrital charcoal and therefore a reliable estimate of terrace age.

[20] On Terrace 3 the soil had a 28-cm-thick dark grayish brown A horizon above a subsoil that graded from 7.5YR hues to 5YR hues with depth. Texture was silt loam and structure was moderately well developed. Importantly, below 68 cm depth, discontinuous clay cutans were common on ped faces and we identified an Argillic (Bt) horizon. The allocation of this pedon to a soil order is equivocal at this stage without base saturation data, but it would be either an Alfisol or an Ultisol.

[21] The soil on Terrace 4 had a dark brown, strongly structured silt loam A horizon over a subsoil with 5YR hue. A disjoint distribution of clay cutans in the depth increments 28–42 cm and 75–120 cm, and crude stratification of clasts in the soil suggests a composite character to the profile. The size range and angularity of the clasts suggest debris flows from nearby hillslopes may have been deposited on the terrace in the past. Subsoil texture graded from clay loam to silt loam with depth. Soils with this degree of reddening in the Bt horizon are generally recognized as Ultisols.

[22] The soil on the last terrace to retain a significant planar morphology (Terrace 5) was an Ultisol with a 20-cm-thick dark reddish brown A horizon over a subsoil with 2.5YR hue. The A horizon had concentrations of 1–3 mm diameter spherical Fe concretions (pisoliths) and the B horizon was clay loam with a few highly weathered clasts. The pisoliths are evidence of extended periods of weathering in which there is a relative loss of Si with respect to Fe and Al. Clay cutans were common or many, continuous and thick below 50 cm depth.

[23] The soils on the ridgeline steps (Terraces 6 and 7) were both Ultisols with similar characteristics. Both had thin A horizons over silty clay subsoils with hues ranging from 2.5YR to 10R. The reddest hue (10R) appeared to be associated with the abundant thick clay/oxide cutans that coat ped faces in the lower B horizon such that when a pit face was scraped the hue appeared as the slightly less red 2.5YR hue. Unlike all soils on lower terraces, a deep saprolitic zone extended more than 8.0 m (the length of our auger) below the base of the cuttings we described. In both profiles the saprolite was a soft clay with abundant lithorelicts that could be divided into an upper yellow-weathered subzone and a lower pallid subzone typical of lateritic profiles and indicative of long periods of chemical weathering.

[24] In summary, trends in soil properties across the chronosequence from young to old are: an increase in clay content, an increased expression of clay cutans, and an increase in redness. Depth to the base of the B horizon, and depth to the base of weathering also increase (Figure 4 and Table 1). Soil taxa range from composite Entisol/Inceptisol (Terrace1), to Inceptisol (Terrace 2) to Alfisol or Ultisol (Terrace 3) to Ultisol (Terraces 4 and higher).

[25] Soil hue increases in redness rapidly over the first five terraces, which are separated by 36 m elevation difference (Figure 4a). We fit the soil hue data using equation (10), $r^2 = 0.95$ ($P = 0.0027$). Depth to the base of the B horizon also varies nonlinearly with elevation as does the depth to the base of weathering, although the form of the relationship is undefined owing to the minimum depth estimates for Terraces 6 and 7 (Figures 4b and 4c). Extrapolating a linear relationship based on Terraces 2–5, we might expect weathering extending to ~20 m at Terraces 6 and 7 (Figure 4c). On Terraces 4–7, recognition of the base of the B horizon was problematic because the boundary was identified from auger sampling, which made recognition of soil structure and sedimentary structure difficult because of the intense soil disturbance.

[26] Radiocarbon ages from Terrace 1 indicate that shallow Inceptisols with 10YR hues in the B horizon can form within 1000–2000 years. Determining an incision rate (0.18 ± 0.04 mm yr^{-1}) from the Terrace 2 radiocarbon age (40.2 ± 2 ka cal BP) enabled us to estimate the age and residence time of higher terrace soils on the basis of their relative elevation (Figure 4a).

5.2. Estimating Soil Residence Time

[27] Using soil reddening, as quantified by hue number (H), as our indicator of soil weathering on hillslopes, equation (14) becomes

$$T = \frac{H - H_0}{\lambda[K - (H - H_0)]}, \tag{15}$$

where H_0 is the hue number of the soil at 0 years. Using the parameters of the best fit exponential function to the data in Figure 4a ($H_0 = 1.98$, $\lambda = 6.7 \times 10^{-6}$, $K = 10.53$), the residence time T for soils on a hillslope with soil hue 7.5YR ($H = 5$) is 60 ka.

[28] In contrast, the age of a soil that has parent material of uniform age, such as on a terrace, can be calculated by solving equation (10) for t using the calibrated chronofunc-

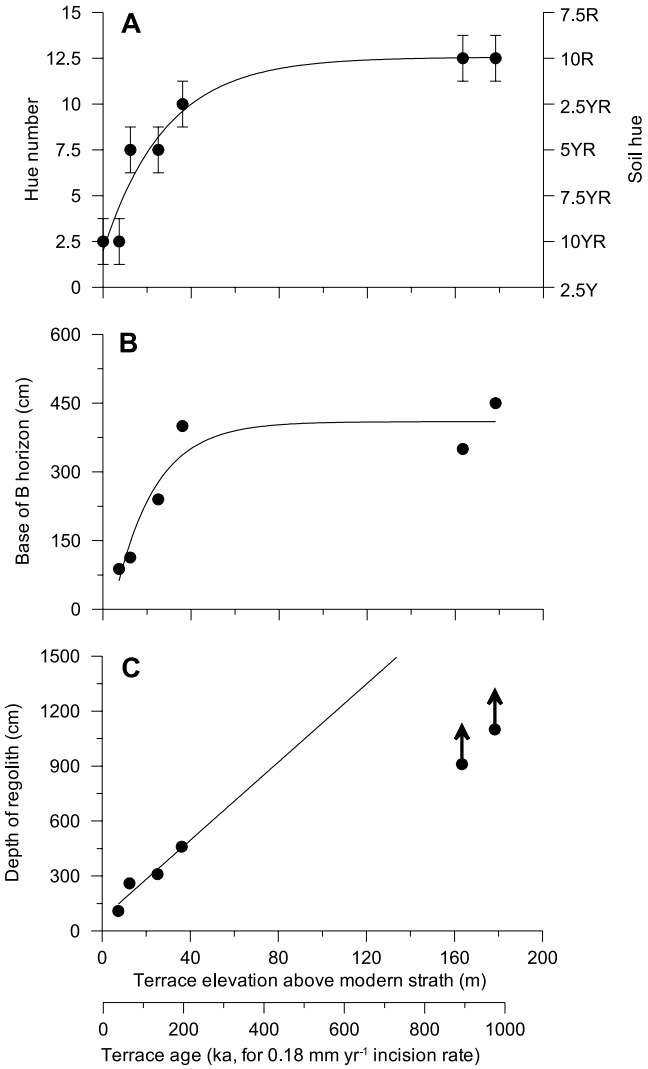

Figure 4. (a–c) Soil chronosequence relationships for the terraces shown in Figure 3. The terrace age axis is calculated using an averaged incision rate of 0.18 mm yr^{-1}, on the basis of radiocarbon dating of detrital charcoal in Terrace 2 (see text). Figure 4a shows the variation of soil hue (and hue number) for the reddest component of the B horizon with terrace age. The solid line is equation (10), where $H_0 = W_0 = 1.98$, $K = 10.53$, $\lambda = 6.7 \times 10^{-6}$, with $r^2 = 0.95$. Figure 4b shows the variation of depth to the base of the B horizon with terrace age. The solid line is equation (10), where $B_0 = W_0 = -107$, $K = 516$, $\lambda = 9.9 \times 10^{-6}$, and $r^2 = 0.89$. Figure 4c shows the variation of depth of regolith with terrace elevation (age). Depth estimates for Terraces 6 and 7 (ages > 800 ka) are minimum values. The solid line is a linear fit to Terraces 2–5 (terraces with age <300 ka). The depth of regolith is 0.00194 * (terrace age) + 69.3, where $r^2 = 0.91$.

tion parameters. For example, the age, t_{age}, of a terrace soil with hue 7.5YR is 50 ka according to

$$t_{age} = -\frac{1}{\lambda} \ln\left[\frac{K - (H - H_0)}{K}\right]. \quad (16)$$

Residence time and soil age calculations for the range of hues encountered in our study area are tabulated in Table 2. Residence time for hillslope soils (T) is larger than soil age (t_{age}) for a given hue number because the particle age distribution for hillslope soils is positively skewed (inset, Figure 1) and the weathering function is nonlinear. The 10 ka difference between T and t_{age} in this example (H = 7.5YR) highlights the potential error in equating soil age based on terrace data to the residence time of soil on steadily eroding hillslopes. Failure to distinguish residence time from soil age results in residence time underestimation and erosion rates overestimation.

5.3. Spatial Patterns of Soil Residence Time

[29] Mapping of residence time involved simply reclassifying soil map units according to B horizon hue (Figure 5a). Below we describe the pattern in terms of soil hue, but it could equally have been done in terms of corresponding residence times (Table 2). The resulting map does not exhibit random variation, but instead reveals systematic patterns with varying spatial scale and geomorphic context. Most obvious is the abundance of 5YR soils in the eastern third of the study area. This rather contiguous zone of weathered soils sharply contrasts with the predominantly 10YR soils that dominate the western portion of the study area. Within that western region, however, we observed locales with concentrated patches of deeply weathered, 5YR soils. Finally, we also observed an abundance of 5YR soil patches along ridges bordering meandering stretches of the Siuslaw River, perhaps reflecting the preservation of old geomorphic surfaces on the inside of migrating meander bends, as exemplified by our chronosequence site (Figure 5a).

[30] To analyze factors that may influence the east-west residence time contrast, we plotted the location of the Long Tom Creek–Siuslaw River drainage divide and noticed a general correspondence such that 5YR soils dominate areas east of the divide and 10YR soils abound to the west (Figure 5b). Although localized patches of 5YR soils do extend west of the divide, the zone of rather contiguous 5YR soils resides wholly within the Long Tom catchment, which drains northeast to the Willamette River. To further illustrate this pattern, we quantified how the proportion of soils with a particular soil hue (i.e., residence time) varies longitudinally by constructing a series of 4.5-km-wide (measured east-west) swaths that spanned the study area

Table 2. Calculated Residence Times for Hillslope Soils and Ages for Soils With Uniform Parent Material Age of Different B Horizon Hue[a]

B Horizon Hue	Hue Number	Residence Time T, ka	Age of Soil t_{age}, ka
10YR	2.5	7.8 ± 5	7.6 ± 5
7.5YR	5	60 ± 34	50 ± 32
5YR	7.5	165 ± 85	111 ± 55
2.5YR	10	478 ± 265	214 ± 120
10R	12.5	2940 ± 1550	453 ± 245

[a]Errors are standard errors estimated using Gaussian error propagation. Residence times are calculated from equation (15), and ages are calculated from equation (16).

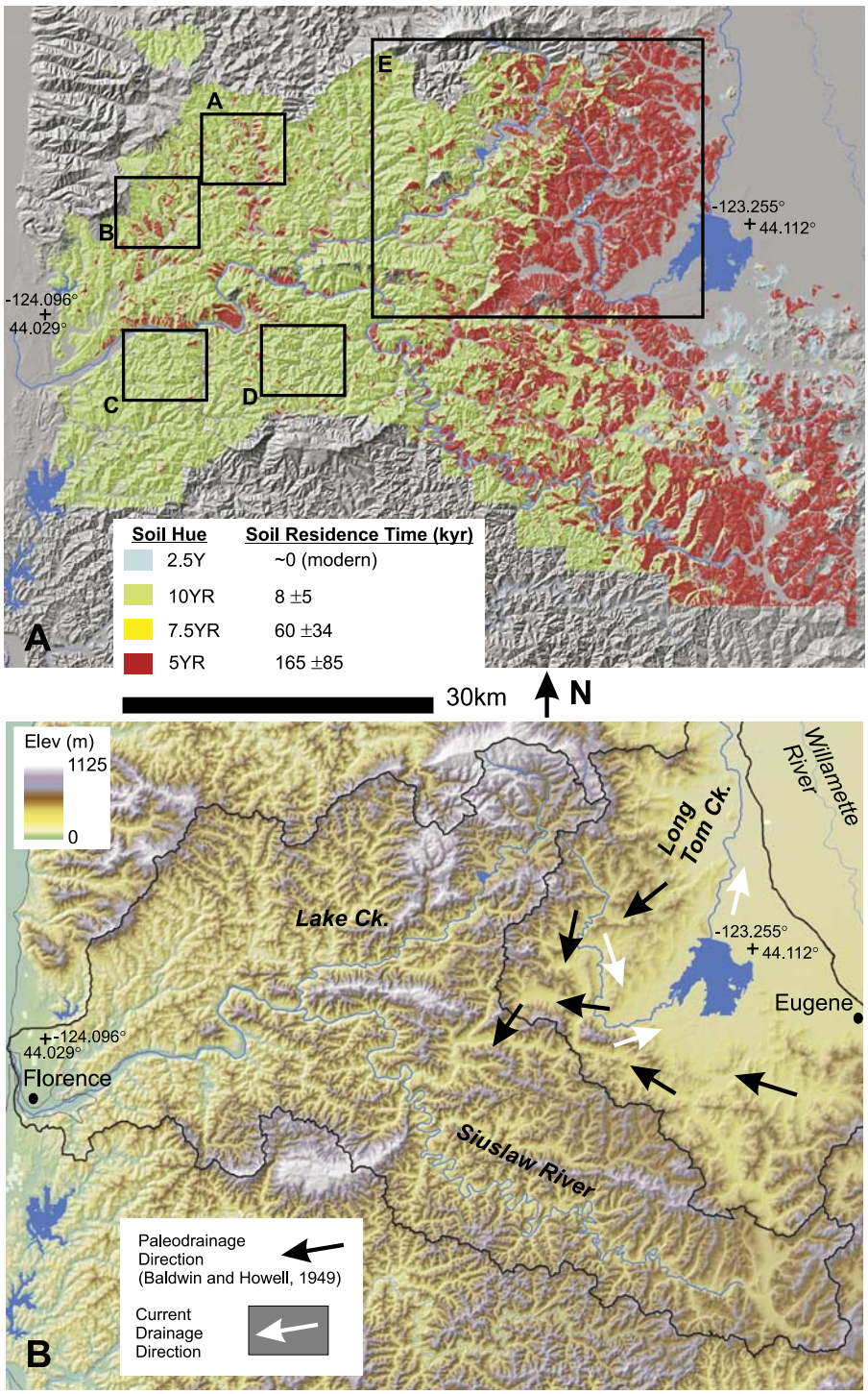

Figure 5. (a) Map of soil hue based on Lane County Soil Survey soil map unit designations for Tyee Formation–derived soils in the Siuslaw drainage basin. Red soils (5YR) are found along the eastern margin of the study area, whereas 10YR soils dominate the western region. Boxes labeled A–D and E refer to sites shown in Figures 8 and 7, respectively. (b) Map of elevation and watershed boundaries for the same area as that shown in Figure 5a. The Siuslaw–Long Tom drainage divide roughly corresponds with the transition in soil characteristics. Arrows show paleo (dark) and current (white) flow directions for the Long Tom River according to *Baldwin and Howell* [1949].

(in the north-south direction) and estimating the fractional area of different soil units contained within each swath (Figure 6). To the west, 10YR soils constitute ~90% of the landscape, although that proportion drops to <30% east of the divide in the Long Tom Creek catchment. This transition does not coincide with changes in climate or lithology. A commensurate increase in the frequency of 5YR soils to the east provides direct evidence of a dramatic increase in soil

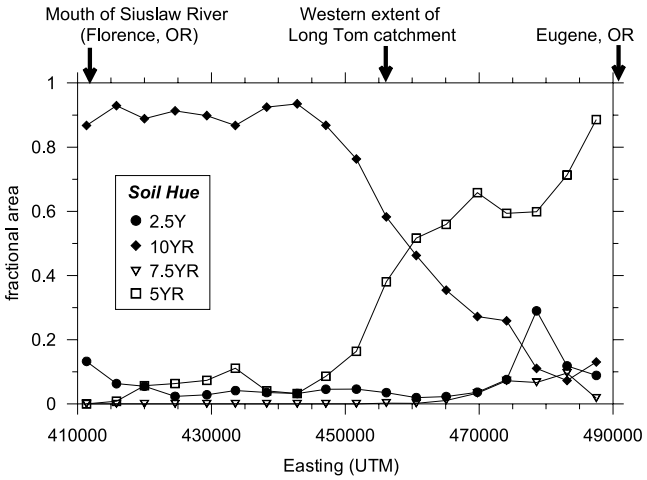

Figure 6. Longitudinal variations in the fraction of soils of different hue shown in Figure 5a. This plot shows the fractional contribution of soils of different hue along a transect oriented perpendicular to the coast from the mouth of the Siuslaw River to Eugene. The 4.5-km-wide (measured east-west) bins were constructed to span the entire study area in the north-south direction (approximately 60 km) and were constructed to exactly adjoin each other on the margins, such that all soil patches shown in Figure 5a are represented. The longitude value at the center of each north-south oriented rectangular swath was used to plot the relevant variations in soil values. No averaging is used; instead, within each bin we calculated the fraction of area composed of soils of different hue as per the soil survey database.

residence time for portions of the Oregon Coast Range that drain into the Willamette Valley.

[31] Because such a significant change in soil characteristics may reflect variations in the rate of transport processes that have topographic dependencies, we calculated the distribution of hillslope angle (measured in percent using a 10 m DEM) for a region surrounding the Long Tom–Siuslaw divide (Figure 7a). To the west, average slope angles for ubiquitous ridge and valley terrain are generally steep (mean = 45%), reflecting rapid rates of channel incision and sediment production (Figure 7b). In contrast, hillslopes within the eastern region are much gentler (mean = 22%) and valleys tend to be much broader, constituting a larger fraction of the landscape. This region of gentle slopes and broad valley floors corresponds with the course of reversed river flow identified by *Baldwin and Howell* [1949] such that much of Long Tom Creek formerly belonged to the Siuslaw drainage basin. This geomorphic transition may reflect a structurally induced stream capture episode although the specific mechanisms are currently equivocal.

[32] In addition, we analyzed concentrated patches of 5YR soils in the western portion of the study site and compared their location to recently identified deep-seated landslides [*Roering et al.*, 2005]. The topographic signature of deep-seated landslides in the region is distinct (see red zones in Figure 8) and these areas coarsely coincide with mapped 5YR soils although the correspondence is certainly not exact. Most generally, it appears that the soil survey [*Patching*, 1987] delineated irregularly shaped patches of highly weathered soil along broad, low-gradient ridges and sideslopes. The exact position of their soil map units often relies on extrapolating point observations using air photos and topographic maps. Large landslides and deeply weathered soils likely correspond in the Oregon Coast Range because slope instability destroys the steep, ridge and valley terrain that is generated and maintained by relatively rapid soil production, transport, and evacuation by debris flows. These physical processes are effectively "switched off" when deep-seated slope instability imposes bench-like morphology on the landscape, enabling chemical weathering to exhibit a stronger imprint in the landscape.

[33] Finally, our map of soil hue consistently reveals large patches of 5YR soils along slopes adjacent to meandering segments of the Siuslaw River (see southern margin of Figure 5a). These weathered soils tend to occur along the inside bank of large bedrock meanders which form in the wake of lateral river migration. Located 10–100 m above the current riverbed, these areas may record the long-term (up to 1 Ma) history of fluvial activity and most generally emphasize the lateral dynamics of bedrock channels. Cutoff bedrock meanders are not uncommon in OCR rivers, indicating significant planform channel adjustments.

6. Discussion

6.1. Soil Variability and Soil Chronosequences

[34] In order to use a chronofunction based on B horizon hue to estimate soil residence time, we must be confident that changes in that property relate to differences in soil age and not other soil forming factors, both in the chronosequence and in the rest of the landscape. In studying a soil chronosequence across fluvial terraces in the Mediterranean climate of the Transverse Ranges in Southern California, *McFadden and Hendricks* [1985] demonstrated that a reddening of the soils with time resulted from a progressive accumulation of Fe oxides and increasing hematite content. They concluded that soil Fe oxide analysis had potential as a chronological tool. *Markewich and Pavich* [1991] also found a consistent trend of reddening with increasing age of Ultisols on the Coastal Plain of the eastern United States. A chronosequence near our study site situated on the marine terraces near Capes Arago and Blanco in southern Oregon also showed a reddening of B horizon with increasing soil age [*LangleyTurnbaugh and Bockheim*, 1997], but pedogenesis there is apparently more complex than at our site. Podzolization and argilluviation (translocation of clay) act concurrently in these soils with relative intensity dependent on terrace age. Accordingly, those soils show characteristics of both Ultisols and Spodosols. The climates and vegetation of the coastal Oregon study and the present study are very similar and why pathways of pedogenesis differ is not clear. Podzolization processes on the marine terraces may be promoted by the coarse-textured, acidic nature of the marine sand parent materials along the coast [*Bockheim et al.*, 1996], whereas the arkosic Tyee formation may buffer against the acidification necessary for mobilization of Fe and Al involved in podzolisation.

[35] Variation in soil color across our chronosequence could also be strongly influenced by past climate changes.

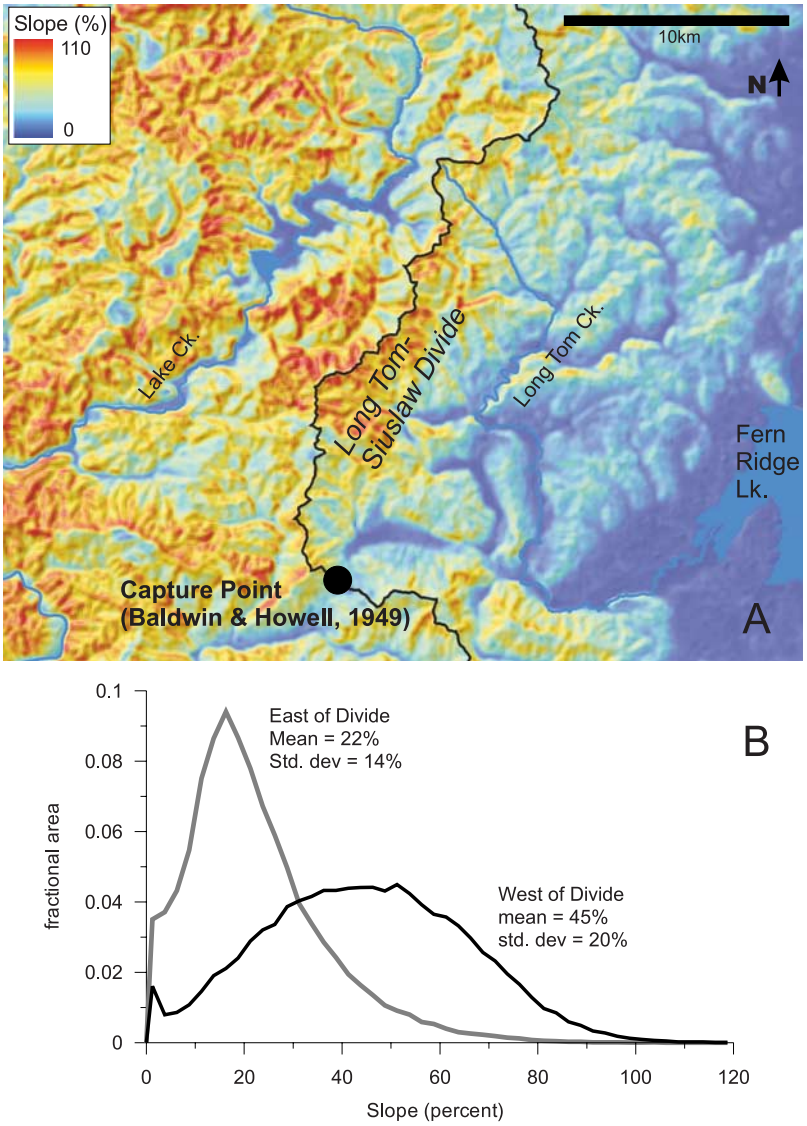

Figure 7. (a) Average slope values (percent) for box E as delineated in Figure 5a. Slope values were averaged using a 50 m radius window to smooth local variability. Gentle slopes in the east area associated with red soils contrast 10YR soils in the west. (b) The distribution of slope values (not averaged) for 10 × 10 km patches of terrain on either side of the drainage divide, illustrating the low-gradient character of the Long Tom catchment in contrast to the steep and dissected terrain of Lake Ck. (tributary of the Siuslaw River).

Hematite, responsible for hues of 5YR and redder, is favored by warm, dry conditions with relatively low organic matter activity. Goethite, which has hues of 2.5Y to 7.5YR, is favored by cooler temperatures, and higher H_2O and organic matter activities [*Schwertmann and Taylor*, 1989]. A 42,000-year climate record for the Central Oregon Coast Range based on pollen shows seven climate transitions to conditions both warmer and colder than present and wetter and drier than present [*Worona and Whitlock*, 1995]. These changes, related to Milankovitch orbital forcing and climate system feedbacks, are frequent enough that all but the youngest soils will have experienced many similar cycles, and therefore we expect that soil properties developed over 10,000- to 100,000-year timescales integrate over numerous short-timescale climate variations. Thus the systematic changes observed in our chronosequence likely reflect temporally derived variations in weathering rather than a sequence of climatically induced process changes.

[36] The validity of extrapolating the terraced-based chronofunction to soil on hillslopes requires further consideration. Hillslope soils form from different parent materials and under different topographic conditions than terrace soils. Although the parent material of soils in our study area ultimately originates from Tyee formation, fluvial sorting of terrace alluvium may cause differences in particle size distribution and mineralogy such that rates or pathways of pedogenesis may differ in hillslope colluvium. We extracted reference pedon descriptions and characterization data from NRCS databases (National soil survey characterization data, Soil Survey Staff, National Soil Survey Center,

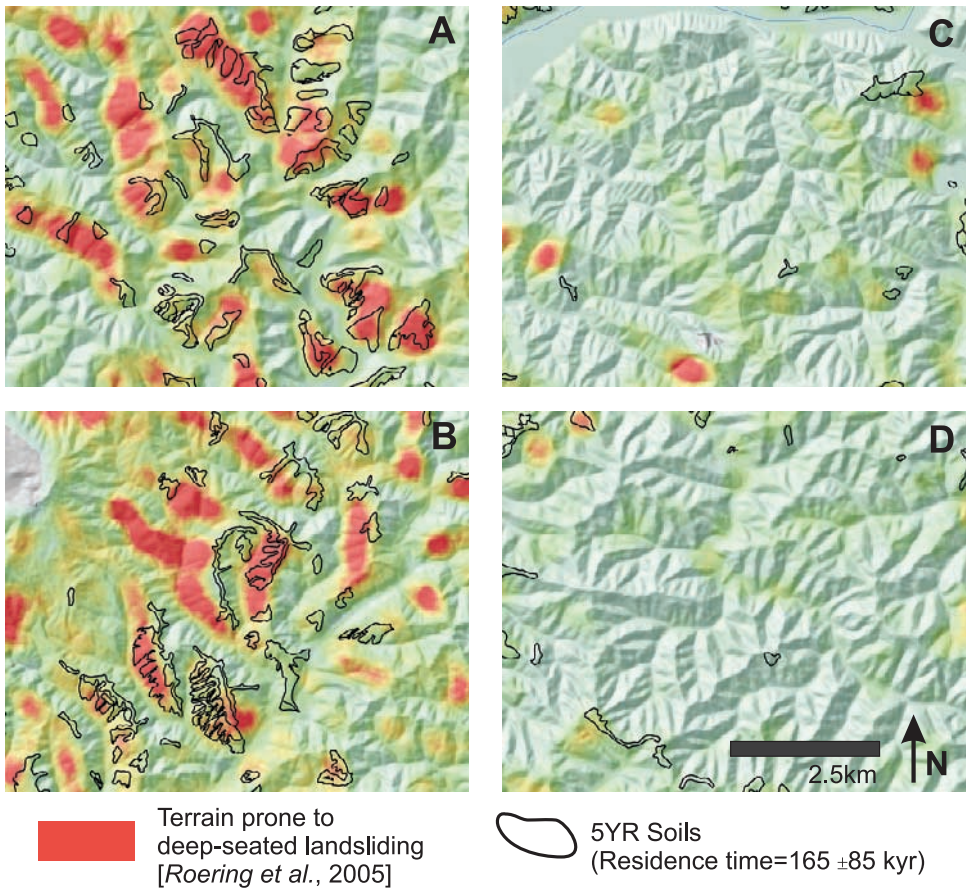

Figure 8. (a–d) Maps of deep-seated landslide-prone terrain (see boxes A–D in Figure 5a). Landslide-prone terrain was estimated from slope and curvature criteria estimated from a digital elevation model [*Roering et al.*, 2005]. Red patches illustrate the calibrated delineation of terrain consistent with deep-seated landsliding. Open polygons represent 5YR soils determined from the Lane County Soil Survey [*Patching*, 1987], as shown in Figure 5a. The general correspondence between large landslides and red soils (Figures 8a and 8b) reflects a process linkage between slope instability and balance of mass removal via physical and chemical processes. In areas with infrequent slide-prone terrain, weathered (5YR) soils are sparse.

Lincoln, Nebraska, 2006, http://ssldata.nrcs.usda.gov/; Official soil series descriptions, Soil Survey Division Staff, Natural Resources Conservation Service, United States Department of Agriculture, Washington, D. C., 2007, http://soils.usda.gov/technical/classification/osd/index.html) for the Nekoma series mapped on floodplains (equivalent to our Terrace 1), and for the Digger, Bohannon and Preacher soils mapped on hillslopes in our study area. Particle size classes for the Nekoma C horizons range from fine sandy loam to loamy sand with 5 to 15% clay and up to 50% gravel. Mineralogy class is described as mixed, which is a default mineralogy class if no other distinctive mineralogical characteristics are present. Essentially, this suggests that no mineral makes up more than 40% of the total mineral assemblage except quartz. The soil does not, however, satisfy the criteria of the siliceous mineralogy class, which has more than 90% resistant minerals in the 0.02 to 2 mm fraction. In the hillslope soils the fine earth in the C horizons ranges from loamy sand to sandy loam, with 4 to 20% clay, although such analyses are biased toward fine grain sizes by the presence of weak (pararock) clasts, which disintegrate during sample preparation. Total clast content for hillslope soils is generally higher than for the Nekoma soil, typically in the 10–55% range, and as high as 80% in the lower C horizons. These soils, previously assigned to the mixed mineralogy class, were reassigned to the isotic class in 1999 when new soil chemical and physical data became available. Isotic refers to the fine earth having chemical and physical properties influenced by the presence of short-range-order secondary minerals such as allophane and ferrihydrite. No detailed analyses are available for the Nekoma series, but we note the Meda soil, formed on alluvial fans, has an isotic mineralogy class. These results suggest, at least to first order, a defensible comparability of soil parent materials on hillslopes and terraces. Nonetheless, the higher proportion of clasts in the hillslope soils would tend to decrease the rate of weathering and thereby result in an underestimation of residence time.

[37] Soil variability related to topographic effects may be caused by catenary differentiation from hillcrest to slope hollow. Soil catenas are conceptually divided into an eluvial zone where losses of material by soil transport or lateral

throughflow dominate, a transeluvial zone where material passes through soils, and an illuvial zone where gains of material dominate [*Hallsworth*, 1965; *Tonkin et al.*, 1977; *Young et al.*, 1977]. These zones correspond with the summit (eluvial zone), shoulder and backslope (transeluvial zone) and footslope and toeslope (illuvial zone) slope elements [*Ruhe*, 1975]. The most marked changes in soil properties and morphology tend to occur across zone boundaries [*Tonkin et al.*, 1977], particularly backslope to footslope/toeslope where concentration of water flow lines in convergent topography can lead to soil saturation and changes in redox potential that have a marked effect on soil color. However, because we have excluded predominant topographic convergent zones in our analysis, the major soil hydrological influence on soil color should also has been removed, although even in hollows it appears to be minor. We expect catenary differentiation along the aerially dominant linear backslopes to be unimportant for the following reasons: (1) Shallow soil/bedrock hydrologic experiments highlight the exceptionally high permeability of soils in the OCR and also demonstrate that saturation is rare, even during significant hydrologic events [*Montgomery et al.*, 1997]. (2) Soil surveyors use a mapping device called soil association to indicate catenary variations on hillslopes [*Brown*, 2005] when map scale does not allow them to be delineated; no soil associations have been mapped in the Lane County soil survey, and we did not observe any catenary patterns in our field observations. (3) The colluvial fills in the topographic hollows studied by *Reneau and Dietrich* [1991] in the OCR were mostly 10YR, but were as red as 5YR in hollow fills that began accumulating greater than 40 ka BP. These findings suggest, firstly, that redox-related effects on soil color are minor even in hollows, and secondly, that hillslope soils develop in a manner and rate not inconsistent with the terrace chronosequence. Catenary effects, if they were significant, would delay color development and result in an underestimation of residence times.

[38] Finally, a contrast in precipitation and/or vegetation is unlikely to account for the significant longitudinal transition in soil properties in our study area. Annual precipitation is ~1 m in the western OCR and decreases to just over 0.75 m in the Long Tom drainage basin [*Daly et al.*, 1997].

6.2. Deriving the Chronofunction

[39] *White and Brantley* [2003] showed from experimental and field studies that the time-dependent rate of silicate weathering is best described by a power function of the form,

$$R = At^b, \tag{17}$$

where R is weathering rate, t is time, and b varies between -1 and 0. The function describing the extent of weathering, W, determined by integrating this rate function over time, is also a power function, but with an exponent varying between 0 and 1. Initially, we fit a power function of this form to derive our B horizon hue chronofunction, but found a systematic misfit for the youngest terraces ($r^2 = 0.8$). An exponential function (equation (10)) provided an improved fit ($r^2 = 0.95$), particularly at the young end of the chronosequence where hue development is most rapid. We adopted this empirical approach because better representation of the data was preferable to imposing a predetermined weathering function on complex weathering behavior. Soil reddening involves the mutually competitive formation of hematite at the expense of goethite [*Schwertmann and Taylor*, 1989], and is therefore unlikely to be able to be represented by a continuous mathematical function describing dissolution only.

6.3. Accuracy of the Soil Survey

[40] The 1:20,000 Lane County Soil Survey is classed as a second-order intensive soil survey. Protocols at this intensity of survey demand that boundaries of delineations are located by field observation complemented with interpretation of remotely sensed data. The content of delineations should be determined by traversing across delineations and sometimes transecting within them. The minimum map delineation size is 1.6 ha [*Soil Survey Division Staff*, 1993]. Comparing the boundaries of the terraces in our chronosequence to the soil map (see Figure 3), we note that Terrace 1 shows reasonable correspondence to a delineation of Nekoma series (Inceptisol). The adjacent delineation of Meda soil series (Inceptisol) incorporates Terraces 2 and 3 and parts of Terraces 1 and 5. The soils we observed across these terraces ranged from Inceptisol to Ultisol. Parts of Terraces 4 and 5 are included in a delineation of Blachly silt loam (Inceptisol), which is meant to occur on hillslopes. Terraces 6 and 7 are mapped within a delineation of Preacher soils (Inceptisol) although the soils at our sites were certainly Ultisols. Clearly the soil map does not resolve the small landforms and sometimes subtle soil changes we were able to locate in our detailed study. The orthophoto on which the soil boundaries were mapped suggests an explanation for some discrepancies; the road we used for access and mapping did not exist at the time of the soil survey. Had it existed, the soil surveyors would have likely identified the same terraces and, at least, not have included Terraces 4 and 5 in a hillslope mapping unit. We conclude that the soil surveyors were not carrying out the level of boundary and delineation content checking the survey intensity suggests, although that is not surprising given the difficulty of access in the steep and densely vegetated terrain. Thus we limit our interpretation of the soil spatial data to patterns of mean residence time over broad areas and are cautious to use it for characterizing soils associated with individual hillslopes.

[41] We also view our residence times as order of magnitude estimates because of uncertainties in terrace ages, the parameter sensitivity of the chronofunction, and the inherent heterogeneity of soil map delineations. Terrace ages are estimated from an incision rate calculated from coverbeds just above the Terrace 2 strath. Similar elevations for the Terrace 1 strath and the active bedrock channel bed, however, indicate that incision has been nil for the last 5000 years, and hence must be episodic by nature. For the relatively young Terrace 2, a slowing of incision for 5000 years would cause a minimum underestimation of incision rate of 15%.

6.4. Drainage Capture Along the Siuslaw–Long Tom Drainage Divide

[42] The pattern of highly weathered soils clustering along the eastern margin of the Siuslaw–Long Tom drain-

age divide serves as a significant and readily identified geomorphic signature of base level change induced by drainage capture. Alternative explanations for soil property variations (such as changes in climate or lithology) cannot explain this pattern. *Baldwin and Howell* [1949], *Moeller* [1990], and *Chylek* [2002] presented geomorphic and topographic evidence for capture of this region by the Willamette Valley although the chronology for such an event is unknown. *Baldwin and Howell* [1949] cited the preponderance of broad, alluviated valleys along the main stem and tributaries of the Long Tom River and reconstructed a tentative precapture channel network geometry (Figure 5b). This network follows the uncharacteristically broad valleys, many of which exhibit thick (>100 m) alluvial fills as revealed by drill cores. Thickening increases to the east and additional drill cores near the Fern Ridge reservoir reveal eastward tilting of Tertiary units, providing a structural constraint for tectonic processes that may have instigated stream capture. The primary capture point (Figure 7a), which is a broad topographic saddle that straddles the Siuslaw–Long Tom divide, is thickly mantled by alluvium, reflecting significant aggradation of the southern Willamette Valley. Our analysis reveals patchy highly weathered soils just west of the Siuslaw–Long Tom divide and in the headwaters of the Siuslaw River; this may reflect transient adjustment of low-order channel systems in this region of the OCR (Figure 5b).

[43] Structural models for interpreting deformation that may have driven stream capture along the Willamette Valley are ambiguous and can be generally classed into two groups: (1) orogenic wedge models and (2) block rotation models. *Brandon* [2004] suggests that the OCR–Willamette Valley margin coincides with the retro–shear margin of an orogenic wedge system fed by accretion along the Cascadia subduction zone. The eastward tilting of undated gravels [*Baldwin and Howell*, 1949] is consistent with this model, although other candidates are feasible. This model may be difficult to reconcile given the lack of significant shortening in the Oregon Coast Range (which is emphasized in the orogenic wedge model) and the absence of an obvious range-bounding structure along the Willamette–Coast Range margin. *Wells et al.* [1998] and *Trehu et al.* [1994] suggest that the OCR is underlain by anomalously thick, accreted oceanic terrane (termed Siletzia) that is currently rotating clockwise with respect to stable North America with a pole of rotation in SE Washington near the Oregon-Idaho border. Recent GPS-derived velocities spanning the OCR-Willamette margin are roughly consistent with this structural model [*McCaffrey et al.*, 2000]. When this observation is coupled with the lack of significant range-front deformation structures, it becomes difficult to argue that deformation along the OCR-Willamette margin is ongoing at a significant rate. Instead, variations in crustal thickness may cause western Oregon to undergo broad-scale folding, such that synclinal development of the Willamette may facilitate the capture of west-flowing Cascade Range river systems (Figure 2).

[44] We suggest that stream capture along the eastern margin of the Oregon Coast Range induced a significant change in base level such that the pace of valley lowering was diminished and even reversed in some areas. Following capture, the evolution of Long Tom Creek has been driven by sediment aggradation and incision in the Willamette Valley rather than base level changes at the Oregon Coast. The dominant response has been widespread aggradation of valleys in the southern Willamette Valley, which causes rates of hillslope transport and erosion to decrease such that soil particles take longer to reach the channel network. Our results appear to have captured this change in soil residence time as well as the morphologic manifestation of this transition (Figure 7).

6.5. Pedogenic Signature of Deep-Seated Landsliding

[45] Our map of soil hue supports the notion that soils record geomorphic processes that have a persistent imprint on landscape morphology. Large landslides previously documented in the OCR tend to correlate with highly weathered soils (e.g., 5YR in this case). The occurrence of thick weathering profiles highlights an altered balance of physical and chemical mass removal. The degree of reddening effectively requires a significant reduction in erosion rate compared to that driven by soil transport processes associated with steep, ridge and valley terrain. Similarly, as streams bevel across the landscape, they leave a wake of low-gradient landforms that are poorly dissected and experience low rates of sediment production before significant relief is developed. Given that soil surveyors incorporate topographic information in their map construction, it is possible that the correspondence of highly weathered soils and low-gradient terrain results from extrapolation of point observations. In essence, the correlations could be an artefact of the soil survey process. Interpreted differently, this correspondence emphasizes geomorphic controls on soil development, particularly in such a landscape not subject to glaciation and significant variations in lithology, precipitation, vegetation, or tectonic forcing. Furthermore, the linkage between estimated soil residence times and specific landforms may enable quantitative analyses of landslide chronology and magnitude-frequency behavior. Assuming the relatively low angle, postlandsliding slopes are essentially inactive, the correspondence of 5YR hue soils with many of these features suggests a phase of landsliding approximately 100 ka (t_{age}, Table 2). If, instead, steady erosion has reestablished on these slopes, then the landslides must be older than the residence time of ~165 ka. This latter age estimate must, however, be qualified by a caveat, discussed below, that arises from a potential violation of our model assumptions in areas of low erosion rate.

6.6. Limitations of Soil-Based Residence Time Estimates

[46] Our hue-based estimate of soil residence time (T = 7.8 ka) exceeds the value derived from equation (7) and published erosion rate and soil depth data reported for the OCR (T = 3 ka, where ρ_r/ρ_s = 2.0, E = 0.1 mm yr^{-1}, and h = 0.6 m). Our estimate is closer to the 5000–6000 year residence time calculated by *Reneau and Dietrich* [1991] using a sediment budget approach. A component of the overestimation is likely to arise from uncertainties in the calibration of our chronofunction, particularly for young soils. For ages younger than 100 ka, the age-hue curve is very steep and subtle changes in function parameters, or the type of function used generate large differences in calculated residence time. The problem is exacerbated by our

index of soil weathering being simplistic and dependent on discrete values. The pairs of soils on Terraces 1 and 2, and Terraces 3 and 4 are clearly different in terms of soil development (Table 1) yet they have the same dominant hue (10YR and 5YR, respectively). Our method's coarse approach to quantifying weathering-related soil changes, particularly when soils are changing rapidly, introduces bias and limits the accuracy of our predicted residence times. Ideally, a more sophisticated weathering index would have been used, but as argued above, the available soil survey data did not justify it. More importantly, the tendency for our approach to overestimate residence time suggests that differences in weathering and color development for clast-rich hillslope and sand-rich terrace soils is likely not significant. Similarly, catenary effects on color development, and consequently on residence time estimates, appear to be relatively unimportant, consistent with previous geomorphic studies [*Reneau and Dietrich*, 1991].

[47] At longer timescales it is likely that residence time using our approach is significantly overestimated, not because of chronofunction calibration problems, but because of a violation of our model assumptions. In areas with soils redder than 7.5YR, we observed chemical and pedogenic alteration extending deep into bedrock. Our model assumes chemical alteration and associated soil processes, such as soil reddening, begin after a particle of unweathered bedrock is detached by physical disruption and incorporated in the transported layer. If slopes are gentle enough, the rate of soil transport is low, and soil thickens to a point whereby the rate of physical denudation of bedrock (soil production in the sense of *Heimsath et al.* [1997]) is less than the rate of downward migration of the chemical weathering front. Under these conditions, saprolite forms [*Anderson et al.*, 2002]. Thereafter the transit times and state of alteration of particles detached from the saprolite are no longer as envisaged in our model such that residence time will be overestimated. Finally, our chronology hinges on the locally established incision rate (0.18 mm yr^{-1}), which is similar to erosion rate estimates in the Oregon Coast Range, although somewhat larger than the commonly observed rate of 0.10–0.15 mm yr^{-1} [*Beschta*, 1978; *Bierman et al.*, 2001; *Heimsath et al.*, 2001b; *Reneau and Dietrich*, 1991]. As such, the uncertainty of our soil residence time estimates may be higher than reported here given the difficulty in constraining temporal variations in fluvial incision.

7. Conclusions

[48] Our results highlight the utility of coupling a process-based framework for soil transport and production on hillslopes with a model for pedogenic alteration. Predictions for soil particle behavior along a steady state hillslope suggest that average soil particle residence time is independent of position along the slope and varies only with average soil depth and erosion rate. As such, in the absence of complicating factors, variations in the degree of soil alteration (e.g, soil reddening) may reflect spatially variable soil residence times. In our Oregon Coast Range study area, we document regional and hillslope-scale variations in soil hue (as documented by soil survey data) and relate the spatial pattern to changes in erosion rate driven by drainage capture, deep-seated landsliding, and lateral channel migration. Establishing a soil chronosequence in our study area enables us to relate soil hue to soil residence time and map the spatial distribution of geomorphic process rates. Geomorphic processes such as drainage capture and large landsliding function over significant timescales, enabling them to impose a systematic imprint on landscape form as well as soil development.

[49] **Acknowledgments.** The first author thanks Lincoln University for funding his study leave at the University of Oregon in the fall of 2005. The authors thank Benjamin Mackey, Suzanne Walther, Sean Bemis, and Reed Burgette for their assistance with fieldwork, including pit digging and topographic surveying. Simon Mudd, Kelin Whipple, and an anonymous reviewer provided excellent comments that truly illuminated an early version of this contribution. J. J. R. was funded by NSF EAR-0309975.

References

Anderson, S. P., W. E. Dietrich, and G. H. Brimhall (2002), Weathering profiles, mass-balance analysis, and rates of solute loss: Linkages between weathering and erosion in a small, steep catchment, *Geol. Soc. Am. Bull.*, *114*(9), 1143–1158.

Baldwin, E. M. (1956), Geologic map of the lower Siuslaw River area, Oregon, *Oil Gas Invest. Map OM-186*, U. S. Geol. Surv., Reston, Va.

Baldwin, E. M., and P. W. Howell (1949), The Long Tom, a former tributary of the Siuslaw River, *Northwest Sci.*, *23*, 112–124.

Benda, L., and T. Dunne (1997), Stochastic forcing of sediment supply to channel networks from landsliding and debris flow, *Water Resour. Res.*, *33*(12), 2849–2863.

Beschta, R. L. (1978), Long-term patterns of sediment production following road construction and logging in the Oregon Coast Range, *Water Resour. Res.*, *14*, 1011–1016.

Bierman, P., and K. Nichols (2004), Rock to sediment: Slope to sea with 10-Be–Rates of landscape change, *Annu. Rev. Earth Planet. Sci.*, *32*, 215–255.

Bierman, P., E. Clapp, K. Nichols, A. Gillespie, and M. Caffee (2001), Using cosmogenic nuclide measurements in sediments to understand background rates of erosion and sediment transport, in *Landscape Erosion and Evolution Modeling*, edited by R. S. Harmon and W. W. Doe, pp. 89–115, Kluwer Acad., New York.

Birkeland, P. W. (1999), *Soils and Geomorphology*, vol. xii, 430 pp., Oxford Univ. Press, New York.

Bockheim, J. G., H. M. Kelsey, and J. G. Marshall (1992), Soil development, relative dating, and correlation of late Quaternary marine terraces in southwestern Oregon, *Quat. Res.*, *37*(1), 60–74.

Bockheim, J. G., J. G. Marshall, and H. M. Kelsey (1996), Soil-forming processes and rates on uplifted marine terraces in southwestern Oregon, USA, *Geoderma*, *73*(1–2), 39–62.

Bolin, B., and H. Rodhe (1973), A note on the concepts of age distribution and transit time in natural reservoirs, *Tellus*, *25*, 58–62.

Brandon, M. T. (2004), The Cascadia subduction wedge: The role of accretion, uplift, and erosion, in *Earth Structure: An Introduction to Structural Geology and Tectonics*, edited by B. A. van der Pliujm and S. Marshak, pp. 566–574, McGraw-Hill, New York.

Brown, D. J. (2005), An historical perspective on soil-landscape modeling, in *Environmental Soil-Landscape Modeling: Geographic Information Technologies and Pedometrics*, edited by S. Grunwald, CRC Press, Boca Raton, Fla.

Bull, W. B. (1991), *Geomorphic Responses to Climatic Change*, vol. xviii, 326 pp., Oxford Univ. Press, New York.

Butler, B. E. (1982), A new system for soil studies, *J. Soil Sci.*, *33*, 581–595.

Chan, M. A., and R. H. Dott (1983), Shelf and deep-sea sedimentation in Eocene forearc basin, Western Oregon-fan or non-fan?, *AAPG Bull.*, *67*, 2100–2116.

Chylek, S. (2002), GIS analysis of Quaternary stream capture in the Eastern Coast Range, western Oregon, B.S. thesis, Univ. of Oreg., Eugene, Oreg.

Daly, C., G. H. Taylor, and W. P. Gibson (1997), The PRISM approach to mapping precipitation and temperature, in *10th Conference on Applied Climatology, Reno, NV*, pp. 10–12, Am. Meteorol. Soc., Boston, Mass.

Dietrich, W. E., and T. Dunne (1978), Sediment budget for a small catchment in mountainous terrain, *Z. Geomorphol., Suppl.*, *29*, 191–206.

Hallsworth, E. G. (1965), The relationship between experimental pedology and soil classification, in *Experimental Pedology*, edited by E. G. Hallsworth and D. V. Crawford, 414 pp., Butterworths, London.

Heimsath, A. M., W. E. Dietrich, K. Nishiizumi, and R. C. Finkle (1997), The soil production function and landscape equilibrium, *Nature*, *388*, 358–361.

Heimsath, A. M., J. Chappell, W. E. Dietrich, K. Nishiizumi, and R. C. Finkel (2001a), Late Quaternary erosion in southeastern Australia: A field example using cosmogenic nuclides, *Quat. Int.*, *83–5*, 169–185.

Heimsath, A. M., W. E. Dietrich, K. Nishiizumi, and R. C. Finkel (2001b), Stochastic processes of soil production and transport: Erosion rates, topographic variation and cosmogenic nuclides in the Oregon Coast Range, *Earth Surf. Processes Landforms*, *26*(5), 531–552.

Heller, P. L., and W. R. Dickinson (1985), Submarine ramp facies model for delta-fed, sand-rich turbidite systems, *AAPG Bull.*, *69*(6), 960–976.

Holliday, V. T. (2006), A history of soil geomorphology in the United States, in *Footprints in the Soil*, edited by B. P. Warkentin, 548 pp., Elsevier, New York.

Jenny, H. (1941), *Factors of Soil Formation: A System of Quantitative Pedology*, vol. xii, 281 pp., McGraw-Hill, New York.

Kelsey, H. M., R. L. Ticknor, J. G. Bockheim, and C. E. Mitchell (1996), Quaternary upper plate deformation in coastal Oregon, *Geol. Soc. Am. Bull.*, *108*(7), 843–860.

LangleyTurnbaugh, S. J., and J. G. Bockheim (1997), Time-dependent changes in pedogenic processes on marine terraces in coastal Oregon, *Soil Sci. Soc. Am. J.*, *61*(5), 1428–1440.

Lovell, J. P. B. (1969), Tyee Formation: Undeformed turbidites and their lateral equivalents: Mineralogy and paleogeography, *Geol. Soc. Am. Bull.*, *80*, 9–22.

Markewich, H. W., and M. J. Pavich (1991), Soil chronosequence studies in temperate to subtropical, low-latitude, low-relief terrain with data from the eastern United States, *Geoderma*, *51*(1–4), 213–239.

McCaffrey, R., M. Long, C. Goldfinger, P. Zwiek, J. Nabelek, C. Johnson, and C. Smith (2000), Rotation and plate locking at the southern Cascadia subduction zone, *Geophys. Res. Lett.*, *27*, 3117–3120.

McFadden, L. D., and D. M. Hendricks (1985), Changes in the content and composition of pedogenic iron oxyhydroxides in a chronosequence of soils in southern California, *Quat. Res.*, *23*(2), 189–204.

McNeill, L. C., C. Goldfinger, L. D. Kulm, and R. S. Yeats (2000), Tectonics of the Neogene Cascadia forearc basin: Investigations of a deformed late Miocene unconformity, *Geol. Soc. Am. Bull.*, *112*(8), 1209–1224.

Mills, H. H. (2005), Relative-age dating of transported regolith and application to study of landform evolution in the Appalachians, *Geomorphology*, *67*(1–2), 63–96.

Milne, J. D. G., B. Clayden, P. L. Singleton, and A. D. Wilson (1995), *Soil Description Handbook*, 157 pp., Manaaki Whenua Press, Lincoln, N.Z.

Mitchell, C. E., P. Vincent, R. J. Weldon, and M. Richards (1994), Present-day vertical deformation of the Cascadia margin, Pacific Northwest, United States, *J. Geophys. Res.*, *99*, 12,257–12,277.

Moeller, B. (1990), Stream capture in the Central Oregon Coast Range and its relationship to tectonic and structural geology, M.S. thesis, Univ. of Oreg., Eugene, Oreg.

Montgomery, D. R. (2001), Slope distributions, threshold hillslopes, and steady-state topography, *Am. J. Sci.*, *301*(4–5), 432–454.

Montgomery, D. R., W. E. Dietrich, R. Torres, S. P. Anderson, J. T. Heffner, and K. Loague (1997), Hydrologic response of a steep, unchanneled valley to natural and applied rainfall, *Water Resour. Res.*, *33*(1), 91–109.

Mudd, S. M., and D. J. Furbish (2006), Using chemical tracers in hillslope soils to estimate the importance of chemical denudation under conditions of downslope sediment transport, *J. Geophys. Res.*, *111*, F02021, doi:10.1029/2005JF000343.

Noller, J. S., J. M. Sowers, S. M. Colman, and K. L. Pierce (2000), Introduction to Quaternary geochronology, in *Quaternary Geochronology: Methods and Applications*, *AGU Ref. Shelf Ser.*, vol. 4, edited by J. S. Noller, J. M. Sowers, and W. R. Lettis, pp. 1–10, AGU, Washington, D. C.

Orr, E. L., W. N. Orr, and E. M. Baldwin (1992), *Geology of Oregon*, 254 pp., Kendall/Hunt, Dubuque, Iowa.

Patching, W. R. (1987), Soil survey of Lane County area, Oregon, report, 369 pp., Soil Conserv. Serv., U.S. Dep. of Agric., Washington, D. C.

Pazzaglia, F. J., and M. T. Brandon (2001), A fluvial record of long-term steady-state uplift and erosion across the Cascadia forearc high, western Washington State, *Am. J. Sci.*, *301*(4–5), 385–431.

Personius, S. F. (1995), Late Quaternary stream incision and uplift in the forearc of the Cascadia subduction zone, western Oregon, *J. Geophys. Res.*, *100*, 20,193–20,210.

Reimer, P. J., et al. (2004), IntCal04 terrestrial radiocarbon age calibration, 0–26 Cal Kyr BP, *Radiocarbon*, *46*, 1029–1058.

Reiners, P. W., T. A. Ehlers, and P. K. Zeitler (2005), Past, present, and future of thermochronology, *Rev. Mineral. Geochem.*, *58*, 1–18.

Reneau, S. L., and W. E. Dietrich (1990), Depositional history of hollows on steep hillslopes, coastal Oregon and Washington, *Natl. Geogr. Res.*, *6*(2), 220–230.

Reneau, S. L., and W. E. Dietrich (1991), Erosion rates in the Southern Oregon Coast Range: Evidence for an equilibrium between hillslope erosion and sediment yield, *Earth Surf. Processes Landforms*, *16*(4), 307–322.

Roering, J. J., J. W. Kirchener, and W. E. Dietrich (1999), Evidence for nonlinear, diffusive sediment transport on hillslopes and implications for landscape morphology, *Water Resour. Res.*, *35*(3), 853–870.

Roering, J. J., J. W. Kirchner, and W. E. Dietrich (2001), Hillslope evolution by nonlinear, slope-dependent transport: Steady-state morphology and equilibrium adjustment timescales, *J. Geophys. Res.*, *106*(B8), 16,499–16,513.

Roering, J. J., J. W. Kirchner, and W. E. Dietrich (2005), Characterizing structural and lithologic controls on deep-seated landsliding: Implications for topographic relief and landscape evolution in the Oregon Coast Range, USA, *Geol. Soc. Am. Bull.*, *117*(5/6), 654–668.

Ruhe, R. V. (1975), *Geomorphology: Geomorphic Processes and Surficial Geology*, 246 pp., Houghton Mifflin, Boston, Mass.

Ruhe, R. V., and C. G. Olson (1980), Soil welding, *Soil Sci.*, *130*, 132–139.

Schwertmann, U., and R. M. Taylor (1989), *Iron Oxides*, *SSSA Book Ser.*, vol. 1, edited by J. B. Dixon and S. B. Weed, 1244 pp., Soil Sci. Soc. of Am., Madison, Wis.

Small, E. E., R. S. Anderson, and G. S. Hancock (1999), Estimates of the rate of regolith production using ^{10}Be and ^{26}Al from an alpine hillslope, *Geomorphology*, *27*, 131–150.

Soil Survey Division Staff (1993), *Soil Survey Manual*, *Handbook 19*, Soil Conserv. Serv., U.S. Dep. of Agric., Washington, D. C.

Stuiver, M., and P. J. Reimer (1993), Extended ^{14}C data base and revised CALIB 3.0 ^{14}C age calibration program, *Radiocarbon*, *3*(1), 215–230.

Tarboton, D. G. (1997), A new method for the determination of flow directions and upslope areas in grid digital elevation models, *Water Resour. Res.*, *33*, 309–319.

Tonkin, P. J., and L. R. Basher (1990), Soil stratigraphic techniques in the study of soil and landform evolution across the Southern Alps, New Zealand, *Geomorphology*, *3*, 547–575.

Tonkin, P. J., A. W. Young, D. A. McKie, and A. S. Campbell (1977), Conceptual models of soil development and soil distribution in hill country, central South Island, New Zealand: part I, The analysis of the changes in soil pattern, *N. Z. Soil News*, *25*, 170–172.

Trehu, A. M., et al. (1994), Crustal architecture of the Cascadia forearc, *Science*, *266*, 237–243.

U. S. Natural Resources Conservation Service (1999), *Soil Taxonomy: A Basic System of Soil Classification for Making and Interpreting Soil Surveys*, 869 pp., U.S. Dep. of Agric., Washington, D. C.

Wells, R. E., C. S. Weaver, and R. J. Blakeley (1998), Fore-arc migration in Cascadia and its neotectonic significance, *Geology*, *26*, 759–762.

Wells, S. G., L. D. McFadden, and J. D. Schultz (1990), Eolian landscape evolution and soil formation in the Chaco dune field, southern Colorado Plateau, New Mexico, *Geomorphology*, *3*(3–4), 517–546.

White, A. F., and S. L. Brantley (2003), The effect of time on the weathering of silicate minerals; Why do weathering rates differ in the laboratory and field?, *Chem. Geol.*, *202*(3–4), 479–506.

Willett, S. D., and M. T. Brandon (2002), On steady states in mountain belts, *Geology*, *30*(2), 175–178.

Worona, M. A., and C. Whitlock (1995), Late Quaternary vegetation and climate history near Little Lake, Central Coast Range, Oregon, *Geol. Soc. Am. Bull.*, *107*(7), 867–876.

Yeats, R. S., E. Graven, K. Werner, C. Goldfinger, and T. A. Popowski (2000), Tectonics of the Willamette Valley, Oregon, *U. S. Geol. Surv. Prof. Pap.*, *1560*, 183–222.

Young, A. W., P. J. Tonkin, D. A. McKie, and A. S. Campbell (1977), Conceptual models of soil development and soil distribution in hill country, central South Island, New Zealand: part II, Chemical and mineralogical properties, *N. Z. Soil News*, *25*, 173–175.

P. Almond, Soil and Physical Sciences Group, Division of Agriculture and Life Sciences, P.O. Box 84, Lincoln University, Lincoln 7647, Canterbury, Christchurch, New Zealand. (almondp@lincoln.ac.nz)

T. C. Hales and J. Roering, Department of Geological Sciences, University of Oregon, Eugene, OR 97403-1272, USA. (thales@uoregon.edu; jroering@uoregon.edu)